Deep Learning-Based Beam Tracking for Millimeter-Wave Communications Under Mobility

Sun Hong Lim, *Member, IEEE*, Sunwoo Kim, *Senior Member, IEEE*, Byonghyo Shim, *Senior Member, IEEE*, and Jun Won Choi, *Member, IEEE*

***Abstract*— In this paper, we propose a deep learning-based beam tracking method for millimeter-wave (mmWave) communications. Beam tracking is employed for transmitting the known symbols using the *sounding beams* and tracking time-varying channels to maintain a reliable communication link. When the pose of a user equipment (UE) device varies rapidly, the mmWave channels also tend to vary fast, which hinders seamless communication. Thus, models that can capture temporal behavior of mmWave channels caused by the motion of the device are required, to cope with this problem. Accordingly, we employ a deep neural network to analyze the temporal structure and patterns underlying in the time-varying channels and the signals acquired by inertial sensors. We propose a model based on long short term memory (LSTM) that predicts the distribution of the future channel behavior based on a sequence of input signals available at the UE. This channel distribution is used to 1) control the sounding beams adaptively for the future channel state and 2) update the channel estimate through the *measurement update step* under a sequential Bayesian estimation framework. Our experimental results demonstrate that the proposed method achieves a significant performance gain over the conventional beam tracking methods under various mobility scenarios.**

***Index Terms*— Millimeter-wave communications, beam tracking, mobility, channel estimation, deep learning, deep neural network, LSTM.**

I. Introduction

MILLIMETER wave (mmWave) communication has attracted significant attention for achieving the continuously increasing data throughput requirement of advanced wireless systems [1]–[3]. However, several challenges should be addressed to enable seamless communication over mmWave-band channels. In particular, the received signal power of mmWave communication systems experiences significant attenuation. A potential solution is to employ directional transmit (Tx) and receive (Rx) beamforming antennas to enhance the signal power. Such beams are formed by appropriately adjusting the phase and amplitude of the signal for each antenna element [4], [5].

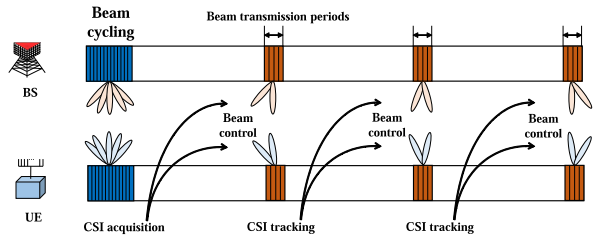

Fig. 1. Illustration of beam tracking protocol.

Consider a base-station (BS) equipped with N_b antennas and a user equipment (UE) with N_m antennas. In down-link scenarios, the BS uses a beamforming vector to transmit the data symbols to the UE and the UE applies a combining vector to receive the transmitted data symbols. These beamforming and combining vectors determine the directions of the beams, which should be chosen to maximize the data throughput. The channel state information should be known to both the BS and UE to determine the directions of the beams. The procedure for acquiring the channel information using pilot symbols is called *beam training*.

In beam training, the pilot symbols are transmitted using specifically designed Tx and Rx beams. These beams are often called *sounding beams* [6]. The BS and the UE use the combinations of M_b Tx sounding beams and M_m Rx sounding beams to obtain the channel information. Consequently, the $M_b \cdot M_m$ pilot symbols are transmitted. Given the absence of prior knowledge about the channel, both M_b and M_m should be sufficiently large to cover a wide range of directions.

Once the initial channel estimate is acquired by the beam training, *beam tracking techniques* are employed to track temporal channel variations using a limited amount of radio resources. When the beam tracking is enabled, the BS transmits the pilot symbols using fewer sounding beams after the initial acquisition step. (see Fig. 1.) The number of sounding

Manuscript received November 30, 2020; revised April 19, 2021 and July 3, 2021; accepted August 13, 2021. Date of publication August 24, 2021; date of current version November 18, 2021. This work was partly supported by Institute of Information & communications Technology Planning & Evaluation (IITP) grant funded by the Korea government (MSIT) (No.2020-0-01373, Artificial Intelligence Graduate School Program (Hanyang University)) and the MSIT under the ITRC (Information Technology Research Center) support program (IITP-2019-2017-0-01637) supervised by the IITP. The associate editor coordinating the review of this article and approving it for publication was F. Gao. *(Corresponding author: Jun Won Choi.)*

Sun Hong Lim, Sunwoo Kim, and Jun Won Choi are with the Department of Electrical Engineering, Hanyang University, Seoul 04763, South Korea (e-mail: shlim@spa.hanyang.ac.kr; romero@hanyang.ac.kr; junwchoi@hanyang.ac.kr).

Byonghyo Shim is with the Department of Electrical and Computer Engineering, Seoul National University, Seoul 08826, South Korea, and also with the Institute of New Media and Communications, Seoul National University, Seoul 08826, South Korea (e-mail: bshim@snu.ac.kr).

Color versions of one or more figures in this article are available at https://doi.org/10.1109/TCOMM.2021.3107526.

Digital Object Identifier 10.1109/TCOMM.2021.3107526

beams can be reduced significantly by exploiting the temporal channel correlation. The BS and UE can use the information on the angles of arrival (AoAs) and angles of departure (AoDs) obtained in the previous beam transmissions to direct only a few beams toward the directions that ensure good channel estimation performance.

Two key design issues exist in implementing beam tracking systems. First, both Tx and Rx sounding beams should be determined in response to the time-varying AoAs and AoDs. Note that such beam control should be predictive to steer the sounding beams toward the future channel state in advance. Second, the UE needs to update the channel estimate by using the received pilot symbols and exploiting the temporal channel correlation.

Various channel tracking methods have been proposed thus far. In [6], the authors proposed a beam tracking algorithm that exploits the temporal correlation between AoDs and AoAs. However, adapting to rapid channel variations was challenging, as omni-directional training beams were used. In [7]–[11], various types of Kalman filters were employed to track time-varying channels. In [12], an optimal beam training protocol design scheme was derived based on the partially observable Markov decision process framework. Compressed sensing (CS) recovery algorithms [13] were also used to estimate the AoDs and AoAs of multi-path channels in [3], [6], [14] and were extended to utilize the temporal channel correlation in [6], [15], [16]. In [17], [18], channel tracking was formulated as a maximum likelihood estimation problem. Sensor-aided beam tracking methods have been proposed recently [19]–[22]. These methods attempted to use an inertial measurement unit (IMU) sensor to assist beam alignment and channel tracking in mmWave systems. However, modeling different types of data acquired from sensor and communication signals to design beam tracking methods is difficult. Thus, applying traditional model-based approaches for sensor-based beam tracking is a significant challenge.

Most UEs are hand-held devices. The pose (i.e., location and orientation) of UE devices can vary based on the motion of their human users. This results in dynamic and instantaneous channel variations. In practice, this could cause frequent beam tracking failures. This necessitates the execution of expensive channel acquisition procedures to recover from failures. Thus, beam tracking algorithms should handle dynamically-varying channels to reduce beam tracking failures and consequently save resource overhead. However, the performance of most existing beam tracking algorithms is limited because they rely on somewhat simple prior linear models to describe time-varying channels. In fact, channels often exhibit structured temporal behavior due to the motion of the UE device. Therefore, channel models that represent such temporal behavior well are required.

Recently, deep neural networks (DNNs) have received considerable attention owing to their ability to find an abstract representation of high-dimensional data [23]. DNNs can model complex non-linear relationships using multiple layers of an artificial neural network. DNNs have achieved state-of-the-art performance in various challenging machine learning tasks. They have been particularly effective for applications in which the existing analytical models cannot adequately describe the distribution of the data. Thus, a DNN can be a suitable candidate for modeling the temporal behavior of mmWave channels caused by the motion of a UE device. Recently, a DNN has been applied for beam training and beam tracking in mmWave systems in [24]–[28]. In [24], convolutional neural networks were used to design hybrid beamformer for wideband multi-carrier mmWave systems. In [25], long-short term memory (LSTM) was used to find an estimate of the angle of arrival (AoA) for the beam tracking algorithm. In [26], the channel state was predicted using LSTM to design a beamformer without using pilot transmission. In [27], online analog beam selection was performed using semi-supervised online learning. Graph neural network was applied to estimate the channel states for massive multi-input multi-output (MIMO) network in [28].

In this paper, we propose an enhanced beam tracking method, that models rapidly-varying mmWave channels using DNNs. We employ a LSTM architecture to describe the temporal evolution of the AoAs and AoDs, using the information available in a UE device. Specifically, the LSTM predicts the distribution of the AoA and AoD states for the current beam transmission cycle based on the sequence of the previous channel estimates and IMU sensor signals. This distribution is used for two main beam tracking operations. First, the distribution of the AoAs and AoDs is used to determine the Rx and Tx sounding beams to be used in the current beam transmission cycle. Second, the predicted channel distribution is used as prior information to update the channel estimate. The proposed LSTM-based prediction model is incorporated into a sequential Bayesian estimation framework, in which the channel information is updated through a *prediction update step* and *measurement update step* in an alternating manner. Note that the proposed method uses the LSTM-based prediction model to update the channel distribution in the prediction update step. This distribution is then used as the prior channel information in the subsequent measurement update step. We evaluate the performance of the proposed beam tracking method via computer simulation. Our results demonstrate that the proposed method achieves significant performance gains over conventional beam tracking methods under various high-mobility scenarios.

The contributions of this paper are summarized as follows;

- Our method uses a DNN to enhance the beam tracking performance in mmWave systems. As compared with widely used simple linear models, the DNN model can capture the complex temporal channel behavior caused by the motion of a device, thereby offering an enhanced beam tracking performance. The superiority of the proposed DNN-based beam tracking scheme over the existing methods is confirmed via numerical evaluation.
- The main idea of this manuscript is to employ deep learning framework to analyze the channel dynamics and predict the future channel state under Bayesian filtering framework. We incorporate the DNN-based prediction model into the sequential Bayesian filtering framework. Note that the role of machine learning models is restricted to modeling the temporal behavior of channels only

and we use the analytical model describing the relation from the transmitted beam to the received signal in the measurement update step. This is consistent with the design principles of respecting established models for well-known physical processes and using data-driven approaches only where the actual physical process is barely known (e.g., temporal channel evolution under mobility environment). This approach contrasts with the end-to-end modeling of beam tracking proposed in [25].

- Recently, a DNN-based channel tracking has been proposed in [25]. The method in [25] directly estimates the AoA using the DNN, whereas the proposed method predicts the future distribution of AoA. The predicted AoA information is then used to update the channel estimate based on the measurement model.

II. mmWave Beam Tracking Systems

In this section, we describe the mmWave channel model and introduce the widely used beam tracking protocol.

A. mmWave Channel Model

Recall that the BS and UE have antenna arrays of sizes N_b and N_m, respectively. The downlink channel from the BS to the UE can be expressed as the matrix $\mathbf{H}_t$ of size $N_m \times N_b$, where the (i,j)th element of $\mathbf{H}_t$ represents the channel gain from the jth antenna of the BS to the ith antenna of the UE. The subscript t represents the tth beam transmission period. The channel $\mathbf{H}_t$ is assumed to be constant within the tth beam training period. The mmWave channel can be represented in the angular domain as [3], [14]

$$\mathbf{H}_t = \sum_{l=1}^{L} \alpha_{l,t} \mathbf{a}^{(m)}(\theta_{l,t}^{(m)}) \left(\mathbf{a}^{(b)}(\theta_{l,t}^{(b)})\right)^H, \tag{1}$$

where L is the total number of paths, $\alpha_{l,t}$ is the channel gain for the lth path, and $\theta_{l,t}^{(b)}$ and $\theta_{l,t}^{(m)}$ are the AoD and AoA, respectively. The AoD and AoA are obtained from $\theta_{l,t}^{(b)} = \sin(\phi_{l,t}^{(b)})$, $\theta_{l,t}^{(m)} = \sin(\phi_{l,t}^{(m)})$, where $\phi_{l,t}^{(b)}$ and $\phi_{l,t}^{(m)} \in [-\frac{\pi}{2}, \frac{\pi}{2}]$ are the AoD and AoA in radians, respectively. The steering vectors $\mathbf{a}^{(b)}(\theta)$ and $\mathbf{a}^{(m)}(\theta)$ are expressed as

$$\mathbf{a}^{(b)}(\theta) = \frac{1}{\sqrt{N_b}} \left[1, e^{\frac{j2\pi d_b \theta}{\lambda}}, e^{\frac{j2\pi 2 d_b \theta}{\lambda}}, \ldots, e^{\frac{j2\pi (N_b-1) d_b \theta}{\lambda}}\right]^T$$

$$\mathbf{a}^{(m)}(\theta) = \frac{1}{\sqrt{N_m}} \left[1, e^{\frac{j2\pi d_m \theta}{\lambda}}, e^{\frac{j2\pi 2 d_m \theta}{\lambda}}, \ldots, e^{\frac{j2\pi (N_m-1) d_m \theta}{\lambda}}\right]^T,$$

where d_b and d_m are the distances between adjacent antennas for the BS and UE, respectively and λ is the signal wavelength. In practical scenarios, L tends to be small, because only a few paths exhibit dominant energy Note that the mmWave channel is determined by the set of parameters $[\alpha_{1,t}, \theta_{1,t}^{(m)}, \theta_{1,t}^{(b)}, \ldots, \alpha_{L,t}, \theta_{L,t}^{(m)}, \theta_{L,t}^{(b)}]^T$.

B. Beam Tracking Protocol

Fig. 1 illustrates a typical beam tracking protocol. For the initial channel acquisition, *beam training* is performed without prior knowledge about the channel. Since CSI information is not available, beam training uses Tx and Rx sounding beams distributed over a wide range of directions, and does not utilize the temporal correlation of the channels for channel estimation [3], [29]–[34]. Once the initial channel acquisition is completed, the beam tracking mode starts. At the tth beam transmission period, the beam tracking method uses the channel knowledge to transmit the pilot symbols using significantly fewer sounding beams directed at certain desired directions. After beam transmission, the UE updates the channel estimate based on the measurements. These channel estimates are fed back to the BS through a feedback channel or used for data demodulation. This beam tracking procedure is repeated in each beam transmission cycle. A similar protocol is observed in the 5G standard, where the SS-burst slot and CSI-RS slot are reserved for the initial channel acquisition and beam tracking, respectively [35].

C. mmWave Channel Estimation

At the tth beam transmission, the BS transmits $M_b \cdot M_m$ pilot symbols to the UE using M_b Tx beams and M_m Rx beams. Let $\mathbf{f}_{t,1}, \ldots, \mathbf{f}_{t,M_b}$ represent the beamforming vectors used for the Tx beams and $\mathbf{w}_{t,1}, \ldots, \mathbf{w}_{t,M_m}$ represent the combining vectors for the Rx beams. When an analog beamformer is used, the beamforming and combining vectors are expressed as $\mathbf{f}_{t,i} = \mathbf{a}^{(b)}(\mu_{t,i}^{(b)})$ and $\mathbf{w}_{t,j} = \mathbf{a}^{(m)}(\mu_{t,j}^{(m)})$, respectively, where $\mu_{t,i}^{(b)}$ and $\mu_{t,j}^{(m)}$ are the corresponding directions of the sounding beams. The vector received in the tth beam transmission cycle is expressed as

$$y_{t,(i-1)M_m+j} = \mathbf{w}_{t,j}^H \mathbf{H}_t \mathbf{f}_{t,i} s_{t,i} + n_{t,(i-1)M_m+j}, \tag{2}$$

for $1 \le i \le M_b$ and $1 \le j \le M_m$, where $s_{t,i}$ is the pilot symbol and $n_{t,(i-1)M_m+j}$ is the additive noise. Without losing generality, we let $s_{t,i} = 1$ in the sequel. Note that, for each Tx sounding beam, M_m Rx sounding beams are swept, resulting in $M_m \cdot M_b$ transmissions. Combining the received signals in a vector $\mathbf{y}_t$ as $\mathbf{y}_t = [y_{t,1}, \ldots, y_{t,M_bM_m}]^T$ and using the angular channel representation in (1), we obtain

$$\mathbf{y}_t = \mathrm{vec}(\mathbf{W}_t^H \mathbf{H}_t \mathbf{F}_t) + \mathbf{n}_t, \tag{3}$$

$$= \mathrm{vec}\left(\sum_{l=1}^{L} \alpha_{l,t} \mathbf{W}_t^H \mathbf{a}^{(m)}\left(\theta_{l,t}^{(m)}\right)\left(\mathbf{a}^{(b)}(\theta_{l,t}^{(b)})\right)^H \mathbf{F}_t\right) + \mathbf{n}_t, \tag{4}$$

where $\mathrm{vec}(\cdot)$ is the vectorization operation,[1] $\mathbf{n}_t = [n_{t,1}, \ldots, n_{t,M_bM_m}]^T$, $\mathbf{W}_t = \left[\mathbf{w}_{t,1} \ldots \mathbf{w}_{t,M_m}\right]$, and $\mathbf{F}_t = \left[\mathbf{f}_{t,1} \ldots \mathbf{f}_{t,M_b}\right]$. We assume that the channel gains $\alpha_{1,t}, \ldots, \alpha_{L,t}$ vary slowly so that they can be assumed as being estimated accurately. For specified $\mathbf{F}_t$ and $\mathbf{W}_t$, the channel estimation problem is equivalent to the determination of the set of parameters $\gamma_t = [\gamma_{1,t}^T, \ldots, \gamma_{L,t}^T]^T = [[\theta_{1,t}^{(m)}, \theta_{1,t}^{(b)}], \ldots, [\theta_{L,t}^{(m)}, \theta_{L,t}^{(b)}]]^T$. Accordingly, we formulate the following state-space equation:

- State evolution model

$$\gamma_t = \mathbf{A}_t \gamma_{t-1} + \mathbf{v}_t, \tag{5}$$

[1]For example, $\mathrm{vec}\left(\begin{bmatrix} 1 & 2 \\ 3 & 4 \end{bmatrix}\right) = [1,3,2,4]^T$.

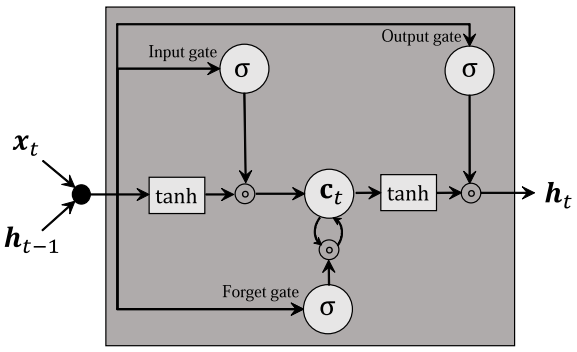

Fig. 2. Structure of the basic LSTM model.

where $\mathbf{A}_t$ is the auto-regressive parameter and $\mathbf{v}_t$ is a complex Gaussian vector $CN(0, V_t)$.

- Measurement model

$$\mathbf{y}_t = \mathrm{vec}\left(\sum_{l=1}^{L} \alpha_{l,t}\mathbf{W}_t^H \mathbf{a}^{(m)}\left(\theta_{l,t}^{(m)}\right)\left(\mathbf{a}^{(b)}(\theta_{l,t}^{(b)})\right)^H \mathbf{F}_t\right) + \mathbf{n}_t. \quad (6)$$

Owing to the nonlinearity of the state-space equation, we can use nonlinear Bayesian filtering algorithms. A popular method used in this regard is the extended Kalman filter (EKF) [7], [8]

1) Prediction update step

$$\begin{aligned}\hat{\gamma}_{t|t-1} &= \mathbf{A}_t\hat{\gamma}_{t-1|t-1}\\ \mathbf{P}_{t|t-1} &= \mathbf{A}_t\mathbf{P}_{t-1|t-1}\mathbf{A}_t^H + \mathbf{V}_t,\end{aligned} \quad (7)$$

2) Measurement update step

$$\begin{aligned}\mathbf{K}_t &= \mathbf{P}_{t|t-1}\mathbf{O}_t^H\left(\mathbf{O}_t\mathbf{P}_{t|t-1}\mathbf{O}_t^H + \sigma_t^2 I\right)^{-1}\\ \mathbf{P}_{t|t} &= (I - \mathbf{K}_t\mathbf{O}_t)\mathbf{P}_{t|t-1}\\ \widehat{\gamma}_{t|t} &= \widehat{\gamma}_{t|t-1} + \mathbf{K}_t\left(\mathbf{y}_t - q(\widehat{\gamma}_{t|t-1})\right),\end{aligned} \quad (8)$$

where the vector $q(\gamma_t)$ and Jacobian matrix $\mathbf{O}_t$ are expressed as

$$q(\gamma_t) = \sum_{l=1}^{L}\mathrm{vec}\left(\alpha_{l,t}\mathbf{W}_t^H\mathbf{a}^{(m)}\left(\theta_{l,t}^{(m)}\right)\left(\mathbf{a}^{(b)}(\theta_{l,t}^{(b)})\right)^H\mathbf{F}_t\right)$$

$$\mathbf{O}_t = \left.\frac{\partial q(\gamma_t)}{\partial \gamma_t}\right|_{\gamma_t=\hat{\gamma}_{t|t-1}}.$$

The expression for $\mathbf{O}_t$ is provided in Appendix A. As the prior channel model in (5) captures only the first-order dynamics of channel variations, EKF often fails to track the complex channel dynamics in the prediction update step, resulting in a large linearization error in the measurement update step.

III. Review of LSTM Model

The LSTM is a DNN architecture widely used to analyze time-series data. Fig. 2 depicts the structure of the LSTM. The LSTM uses recurrent connections to extract features from sequence data and stores them in a memory called *cell state*. When unfolded in time, the connection from the input to the output in the LSTM is deep in time. This enables an efficient representation of long sequences. The LSTM has been successfully applied to various machine-learning problems, e.g., natural language processing, speech recognition, and machine translation. The LSTM consists of a cell state, and input, output, and forget gates. The input, output, and forget gating functions can control the information flows entering and leaving the cell state. These gating functions are designed to address the *vanishing gradient problems*, in which the gradient signals attenuate considerably in learning long-term dependency [36]. Whenever the input x_t is fed into the LSTM, the cell state c_t at the time step t is updated according to the following recursive equations

$$i_t = \sigma(W_{xi}x_t + W_{hi}h_{t-1} + b_i) \quad (9)$$

$$f_t = \sigma(W_{xf}x_t + W_{hf}h_{t-1} + b_f) \quad (10)$$

$$o_t = \sigma(W_{xo}x_t + W_{ho}h_{t-1} + b_o) \quad (11)$$

$$g_t = \tanh(W_{xc}x_t + W_{hc}h_{t-1} + b_c) \quad (12)$$

$$c_t = f_t \odot c_{t-1} + i_t \odot g_t \quad (13)$$

$$h_t = o_t \odot \tanh(c_t), \quad (14)$$

where

- $\sigma(x) = \frac{1}{1+e^{-x}}$: sigmoid function
- $a \odot b$: element-wise product
- W_{xi}, W_{hi}, W_{xf}, W_{hf}, W_{xo}, W_{ho}, W_{xc}, W_{hc}: weight matrices for linear transformation
- b_i, b_f, b_o, b_c: bias vector
- i_t: input gating vector
- f_t: forget gating vector
- o_t: output gating vector
- g_t: state update vector
- h_t: output hidden state vector.

The output h_t of the LSTM contains the feature required to perform the specified task. The desired output can be determined from the feature h_t through an additional neural network. The LSTM is trained to minimize the appropriately designed loss function using the back-propagation through time (BPTT) algorithm.

IV. Proposed Deep Learning-Based Beam Tracking

In this section, we describe the proposed beam tracking method. The proposed method is designed based on the sequential Bayesian filtering framework. We aim to improve the prediction update step in (7) using the machine learning model while retaining the measurement update step in (8). Specifically, we employ the LSTM model to produce the predicted state estimate and the predicted covariance matrix for the prediction update step. The structure of the overall system is depicted in Fig. 3. The LSTM-based prediction model predicts the distribution of the channel state at the tth beam training period based on all the previously available channel estimates and IMU sensor signals. The prediction model produces the mean and covariance matrix of the channel estate separately for each path. Note that the parameters of each model are shared among L paths. Although our algorithm is derived under the assumption that the number of channel

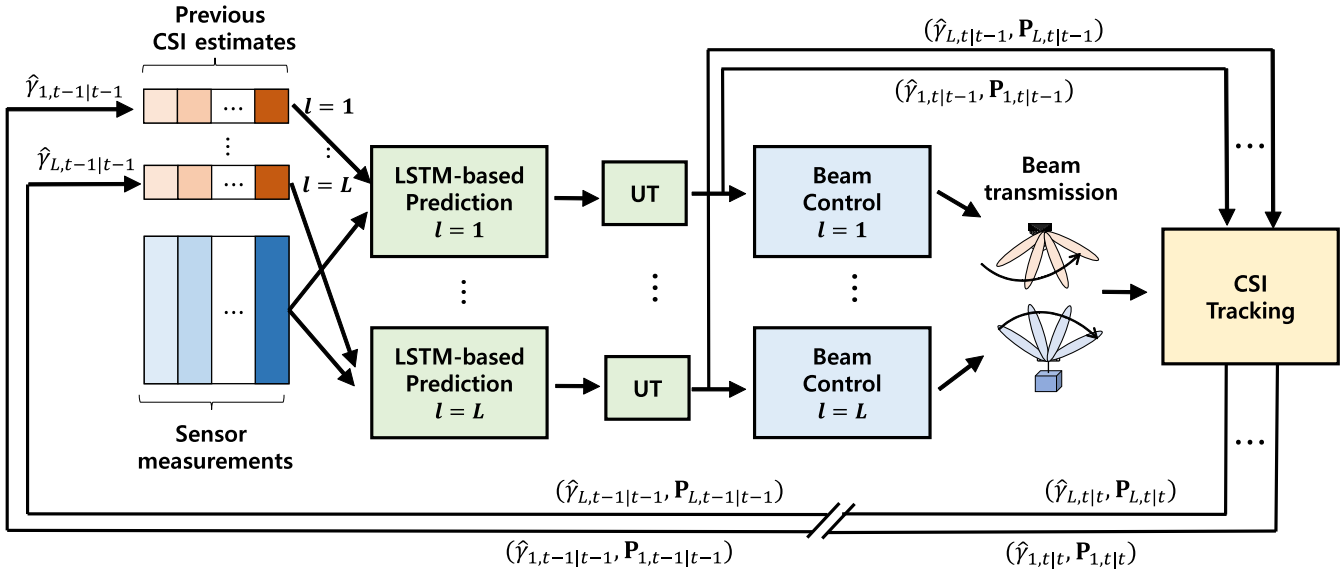

Fig. 3. Block diagram of the proposed beam tracking method.

paths is known, it should be separately estimated in the initial channel acquisition step. After transmitting multiple sounding beams in various directions, the number of channel paths can be estimated based on the received beams using subspace methods such as MUSIC algorithm [37] or correlation-based thresholding methods [16], [29]. As shown in Fig. 3, the output of the prediction model is used to steer both Tx and Rx sounding beams and update the channel estimates based on the received beams.

A. LSTM-Based Channel Prediction

The input to the LSTM-based prediction model includes

- $\hat{\gamma}_{l,t-\delta:t-1} = \left[\hat{\gamma}_{l,t-\delta}^T, \ldots, \hat{\gamma}_{l,t-1}^T\right]^T$: the sequence of the previous δ channel estimates acquired before the tth beam transmission period begins.
- $s_{t-\delta:t-1} = [s_{t-\delta}^T, \ldots, s_{t-1}^T]^T$: s_{t-i} refers to the sample captured by the IMU sensor at the time step $t-i$. In practical applications, IMU sensors measure the velocity, acceleration, angular velocity, and angular acceleration through the accelerometer and gyroscope. Because most advanced UEs are equipped with IMU sensors, the proposed method can use any signals available for beam tracking. As the sampling frequency of these signals can be different from that of the beam transmissions, the sensor signals can be resampled to produce K samples for each beam transmission cycle. Finally, the vector s_{t-i} is filled with $K\delta$ signal samples.
- $\mathcal{C}_t$: the context vector $\mathcal{C}_t$ reflects the UE's situation including activity, location information (indoor vs. outdoor), and channel characteristics. Although it does not represent sequential data, contextual information provides supplementary information on the channels.

The proposed prediction model aims to determine the distribution $p(\gamma_{l,t}|\hat{\gamma}_{l,t-1:t-\delta}, s_{t-1:t-\delta}, \mathcal{C}_t)$ for each channel path for the given past channel estimates $\hat{\gamma}_{l,t-\delta:t-1}$, sensor signals $s_{t-\delta:t-1}$, and context information $\mathcal{C}_t$. We employ the LSTM to model the dependencies between the input and the future channel state. To cope with different channel dynamics under various contexts, we use the UE's contextual information $\mathcal{C}_t$ as an input to the LSTM, where the embedding vector $\mathcal{C}_t$ encodes the situation of UE, e.g., indoor/outdoor location, speed, and activity. By including this information, the LSTM can adapt to changing environments. The UE's contextual information vector $\mathcal{C}_t$ can be encoded appropriately depending on the format of the input. For example, one-hot encoding can be used to represent individual states of UE's situations. User's activity can be encoded as 00: stationary, 01: walking, 10: running, and 11: driving. For location information, we can use 00: indoor, 01: outdoor, 10: traffic road, and 11: subway, for instance. We can also use the number of multi-paths as model input to take advantage of channel properties for prediction. All these contextual information vectors are concatenated to form $\mathcal{C}_t$, which can be further encoded through an additional fully connected layer.

The structure of the LSTM-based prediction model is depicted in Fig. 4. The signal samples $\{\hat{\gamma}_{l,t-\delta}, s_{t-\delta}, \mathcal{C}_t\}, \ldots, \{\hat{\gamma}_{l,t-1}, s_{t-1}, \mathcal{C}_t\}$ are encoded separately by the *input fully-connected (Fc) layers*, i.e.,

$$\nu_{l,t-i} = \mathrm{Fc}(\{\hat{\gamma}_{l,t-i}, s_{t-i}, \mathcal{C}_t\}), \tag{15}$$

where $\nu_{l,t-i}$ is the embedding vector obtained by the Fc layers. The embedding vectors are fed to the LSTM one by one to update the cell state. After δ update of the LSTM, the output h_t is fed into the *output Fc layers* to produce the estimate $\hat{\gamma}_{l,t}$. That is,

$$\hat{\gamma}_{l,t} = \mathrm{Fc}\left(\mathrm{LSTM}\left(\{\nu_{l,t-\delta}, \ldots, \nu_{l,t-1}\}\right)\right). \tag{16}$$

The parameters of the LSTM and Fc layers are determined in the training procedure. In practice, the training data could be collected by deploying several reference UEs, which log the channel states and sensor signals in real scenarios. The

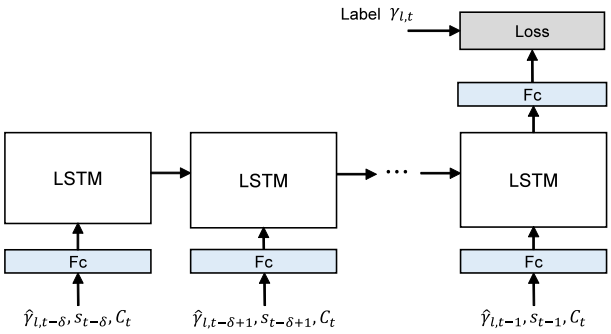

Fig. 4. Structure of the LSTM-based prediction model.

model is trained to minimize the negative log-likelihood loss $\sum \|\gamma_{l,t} - \hat{\gamma}_{l,t}\|^2$, where the ground truth $\gamma_{l,t}$ can be obtained directly from the training data. The prediction network is trained using the standard BPTT algorithm with the ADAM optimization [38]. The model weights are updated over a mini-batch of size *MINIBATCH*. The training starts with the initial learning rate *LEARNING_RATE*. The learning rate decays by half in each *DECAY_EPOCH* epochs. Note that the model is trained over a total of *TOTAL_EPOCH* epochs.

It is worth mentioning that in practical applications, channel evolution tendency might significantly change over time depending on the scenario (e.g., when the user walks or when the user drives a car). In this case, we can consider clustering the context vector $\mathcal{C}_t$ and training the multiple LSTM models for each centroid of the clusters. This allows us to switch between the weights of the LSTM model trained under various contexts.

B. Channel Tracking

The sequential Bayesian estimation framework is widely used to estimate time-varying channels. The Bayesian principle involves updating the distribution of a channel based on all the information available at each step. By adopting this principle, we update the mean $\widehat{\gamma}_{l,t-1|t-1}$ and the covariance matrix $\mathbf{P}_{l,t-1|t-1}$ by $\widehat{\gamma}_{l,t|t-1}$ and $\mathbf{P}_{l,t|t-1}$ through the prediction update step. Subsequently, the measurement update step updates $\widehat{\gamma}_{l,t|t-1}$ and $\mathbf{P}_{l,t|t-1}$ by $\widehat{\gamma}_{l,t|t}$ and $\mathbf{P}_{l,t|t}$. In the prediction update step, the LSTM-based prediction model is used to obtain $\widehat{\gamma}_{l,t|t-1}$ and $\mathbf{P}_{l,t|t-1}$. As the LSTM-based prediction model produces the point estimate of the future channel state, we employ the unscented transformation (UT) [9], [39] to obtain the distribution.

First, for given $\widehat{\gamma}_{l,t-1|t-1}$ and $\mathbf{P}_{l,t-1|t-1}$, we generate $2P+1$ sigma vectors χ_i with the corresponding weights w_i, i.e.,

$$\chi_0 = \widehat{\gamma}_{l,t-1|t-1} \tag{17}$$

$$\chi_i = \widehat{\gamma}_{l,t-1|t-1} + \left(\sqrt{(L+\lambda)\mathbf{P}_{l,t-1|t-1}}\right)_i \quad i = 1, \ldots, P \tag{18}$$

$$\chi_i = \widehat{\gamma}_{l,t-1|t-1} - \left(\sqrt{(L+\lambda)\mathbf{P}_{l,t-1|t-1}}\right)_{i-P} \quad i = P+1, \ldots, 2P \tag{19}$$

$$w_0^{(m)} = \lambda/(L+\lambda) \tag{20}$$

$$w_0^{(c)} = \lambda/(L+\lambda) + (1-\alpha^2+\beta) \tag{21}$$

$$w_i^{(m)} = w_i^{(c)} = 1/(2(K+\lambda)), \tag{22}$$

where $\lambda = \alpha^2\ P - P$ is a scaling parameter, $\alpha = 10^{-3}$ determines the spread of the sigma points around $\widehat{\gamma}_{t-1|t-1}$, and $\beta = 2$ reflects the prior distribution of $\gamma_{l,t}$. $\left(\sqrt{(L+\lambda)\mathbf{P}_{t-1|t-1}}\right)_i$ is the ith row of the matrix square root. Each sigma vector χ_i is combined with $\widehat{\gamma}_{l,t-\delta|t-\delta}, \ldots, \widehat{\gamma}_{l,t-2|t-2}$ and fed to the LSTM prediction model along with the IMU sensor samples. Accordingly, the LSTM prediction model produces $2P+1$ outputs $\nu_0, \ldots, \nu_{2P}$. Ideally, the $2P+1$ sigma vectors should be generated based on the distribution of δ channel states, which requires estimation of the pair-wise covariance between δ channel states under Gaussian assumption. Unfortunately, adding these steps to the Bayesian filter substantially increases the computational complexity. We approximate the algorithm by generating the sigma vectors only for the last channel estimate. Finally, the updated distribution $\widehat{\gamma}_{l,t|t-1}$ and $\mathbf{P}_{l,t|t-1}$ are obtained by the weighted sums

$$\widehat{\gamma}_{l,t|t-1} = \sum_{i=0}^{2P} w_i^{(m)} \nu_i \tag{23}$$

$$\mathbf{P}_{l,t|t-1} = \sum_{i=0}^{2P} w_i^{(c)} (\nu_i - \widehat{\gamma}_{l,t|t-1})(\nu_i - \widehat{\gamma}_{l,t|t-1})^T. \tag{24}$$

It was shown in [39] that the UT yields approximations that are accurate up to at least the second order, with the accuracy of the third and higher-order moments determined by the selection of α and β. After the prediction update step is completed, the measurement update step is performed to obtain the statistics $\widehat{\gamma}_{l,t|t}$ and $\mathbf{P}_{l,t|t}$ from

$$\begin{aligned} \mathbf{K}_t &= \mathbf{P}_{t|t-1}\mathbf{O}_t^H \left(\mathbf{O}_t \mathbf{P}_{l,t|t-1} \mathbf{O}_t^H + \sigma_t^2 I\right)^{-1} \\ \mathbf{P}_{l,t|t} &= (I - \mathbf{K}_t \mathbf{O}_t)\mathbf{P}_{l,t|t-1} \\ \widehat{\gamma}_{l,t|t} &= \widehat{\gamma}_{l,t|t-1} + \mathbf{K}_t \left(\mathbf{y}_t - q(\widehat{\gamma}_{l,t|t-1})\right). \end{aligned} \tag{25}$$

Note that this measurement update step is equivalent to that of the EKF.

C. Predictive Beam Control

The direction of the sounding beams needs to be determined based on the best available channel information in the tth beam transmission cycle. Before the sounding beams are transmitted, the best available channel information is the statistics $\widehat{\gamma}_{l,t|t-1}$ and $\mathbf{P}_{l,t|t-1}$ obtained using the UT. Based on the Gaussian approximation $p(\gamma_{l,t}|\hat{\gamma}_{l,t-1:t-\delta}, s_{t-1:t-\delta}, \mathcal{C}_t) \approx N(\widehat{\gamma}_{l,t|t-1}, \mathbf{P}_{l,t|t-1})$, we determine the beam angles $\mu_{t,1}^{(b)}, \ldots, \mu_{t,M_b}^{(b)}$ and $\mu_{t,1}^{(m)}, \ldots, \mu_{t,M_m}^{(m)}$, where $\mathbf{f}_{t,i} = \mathbf{a}^{(b)}(\mu_{t,i}^{(b)})$ and $\mathbf{w}_{t,j} = \mathbf{a}^{(m)}(\mu_{t,j}^{(m)})$. The optimal beam angles can be determined by maximizing the expected channel estimation performance with respect to the parameters $\mu_{t,1}^{(b)}, \ldots, \mu_{t,M_b}^{(b)}$ and $\mu_{t,1}^{(m)}, \ldots, \mu_{t,M_m}^{(m)}$. An in-depth study on the optimization of the sounding beams has been presented in [3], [12], [40]. In our previous work [40], the problem of sounding beam adaptation was formulated as a minimization of the Cramer-Rao lower bound (CRLB) of the channel

Algorithm 1 Proposed Beam Tracking Algorithm

1: At the tth beam transmission cycle
2: Input: $\{\widehat{\gamma}_{l,t-\delta|t-\delta}, \ldots, \widehat{\gamma}_{l,t-1|t-1}\}_{l=1,..,L}$ and $\{\mathbf{P}_{l,t-\delta|t-\delta}, \ldots, \mathbf{P}_{L,t-1|t-1}\}_{l=1,...,L}$
3: **Prediction update step:**
4: **for** $l = 1$ to L ... **do**
5: Generate $2P+1$ sigma vectors $\chi_0, \ldots, \chi_{2P}$ according to $\widehat{\gamma}_{l,t-1|t-1}$ and $\mathbf{P}_{l,t-1|t-1}$.
6: Feed $\{\widehat{\gamma}_{l,t-\delta|t-\delta}, \ldots, \widehat{\gamma}_{l,t-2|t-2}, \chi_i\}$ to the LSTM prediction model for $i = 0, \ldots, 2P$.
7: Generate $2P+1$ output samples $\nu_0, \ldots, \nu_{2P}$ by taking the outputs of the LSTM prediction model.
8: Update $\widehat{\gamma}_{l,t|t-1}$ and $\mathbf{P}_{l,t|t-1}$ according to (23) and (24).
9: **end for**
10: **Beam adaptation and transmission:**
11: Determine the directions of the sounding beams using the method in [40] and transmit the beams accordingly.
12: **Measurement update step:**
13: **for** $i = 1$ to L ... **do**
14: Update $\widehat{\gamma}_{l,t|t}$ and $\mathbf{P}_{l,t|t}$ according to (25).
15: **end for**
16: $t \leftarrow t+1$ and go back to line 1.

estimation error over the combinations of beam codebook indices. When only two sounding beams are used for Tx and Rx, i.e., $M_b = M_m = 2$, the optimal beam directions could be determined by a two-dimensional search over the beam codebook. In this study, adopting the method in [40], the CRLB is derived for the given channel distribution $N(\widehat{\gamma}_{l,t|t-1}, \mathbf{P}_{l,t|t-1})$, and the optimal sounding beam angles are determined. With the setup $M_b = M_m = 2$, we choose the values of the beam angles $\mu_{t,1}^{(b)}, \mu_{t,2}^{(b)}, \mu_{t,1}^{(m)}, \mu_{t,2}^{(m)}$ using two-dimensional search. Note that this beam control algorithm moves the group of sounding beams toward the future AoD and AoA directions in advance.

D. Algorithm Summary

The proposed beam tracking algorithm is summarized in Algorithm 1.

V. Experimental Results

In this section, we evaluate the performance of the proposed beam tracking algorithm.

A. Simulation Setup

1) mmWave System Setup: In our simulations, we considered 28GHz frequency band communications with uniform linear array (ULA) antennas whose adjacent elements are spaced by a half wavelength. We considered the communication between a single BS with $N_b = 32$ Tx antennas and a single UE device with $N_m = 32$ Rx antennas. Following the 5G NR standard [35], the symbol duration over which a single beam is transmitted was set to $8.93\mu s$ and 14 symbols are included in each slot of duration $125\mu s$. In the simulations, 4 sounding beams ($M_b = 2$ and $M_m = 2$) were transmitted every T_{CSI} slots. The periodicity of beam transmission T_{CSI} was set to 160 slots based on the 5G NR standard [35]. We use the beam codebook, which contains 64 beams with equally spaced angles. The symbol slots not used for beam tracking were allocated for data transmission. The data symbols in each slot were modulated using binary phase-shift keying (BPSK) modulation. The data precoding and combining matrices were obtained from the left and right singular vectors of the channel matrix associated with the highest singular value, respectively.

2) Mobility Model: We assume that rapid channel variations are mostly caused by dynamic changes in the UE's pose (such as roll, pitch, and yaw) due to the motion of spins or shakes. Thus, in the simulations, we consider the scenarios where the UE rotates in place at the average angular velocity of a_{avg}. This type of motion causes severe changes in AoA and affects the performance of mmWave communications. In contrast, AoD does not change much especially when the UE is far enough away from the BS. We assume that only AoA varies in time according to the following dynamic model:

$$\begin{aligned} a_{l,n} &= (1-\rho)a_{avg} + \rho a_{l,n-1} + w_t \\ \theta_{l,n}^{(m)} &= \theta_{l,n-1}^{(m)} + \Delta t(a_{l,n}), \end{aligned} \tag{26}$$

where n is the slot index, $a_{l,n}$ denotes the angular velocity of AoA for the lth path, $\theta_{l,n}^{(m)}$ denotes the AoA, a_{avg} denotes the average angular velocity of AoA, $\Delta t = 125us$ is the symbol duration, $\rho = 0.9999$ is the auto-regressive (AR) parameter, and $w_t \sim N(0, 0.2(1-\rho^2))$. The angular velocity $a_{l,n}$ is modeled by the AR process, and the AoA $\theta_{l,n}^{(m)}$ is generated by accumulating the velocity. In this work, the angular velocity of AoA is modeled by the AR process. This implies that a second-order dynamic model is used to account for the changes in AoA caused by the UE's movement. Such second-order models have been widely used to describe the behavior of dynamic systems in control and robotics fields.

In our work, we mainly consider the scenarios where the UE changes its pose rapidly while the location of UE in relation to the BS does not change much. Therefore, in these scenarios, the channel changes mostly appear in the AoA, not the channel gain and AoD. Thus, we assume that the channel gain and AoD are constant and known.

The number of paths L was set to 3. The AoAs were generated independently for each path. Fig. 5 shows the change in the AoA and angular velocity with different values of a_{avg}. A higher value of a_{avg} leads to faster motion and consequently more dynamic AoA variations. Note that $a_{avg} = 0.4\pi$ indicates that the UE device rotates in approximately $5\ s$.

3) LSTM-Based Prediction Model: We present the detailed configurations of the proposed prediction model. The length of the input sequence for updating the LSTM was set to $\delta = 3$. Each input vector consists of

- The previous channel estimate
- $K = 4$ samples of angular velocity sensor measurements (rad/s)
- $K = 4$ samples of angular acceleration sensor measurement (rad^2/s).

The IMU sensor measurements were generated by computing the first and second sample derivatives of the AoA and adding

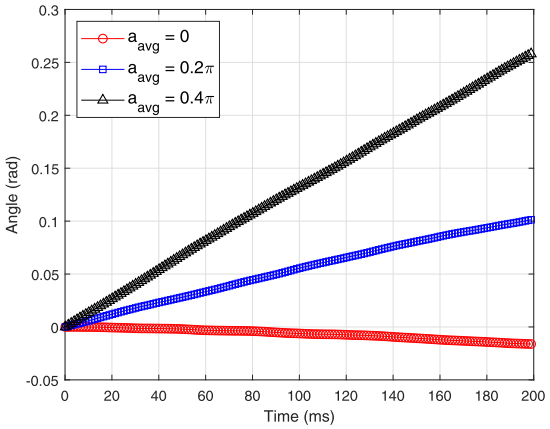

(a)

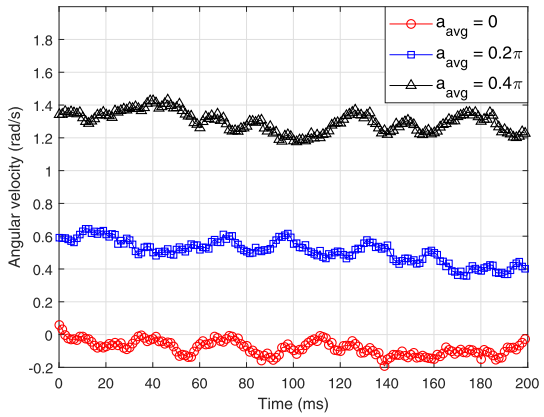

(b)

Fig. 5. Variation of (a) AoA and (b) angular velocity for several values of the parameter a_{avg}.

Gaussian noise. The signal-to-noise ratio (SNR) was set to 5 dB when testing the prediction model. We assume that the IMU sensor has a sampling period $K = 4$ times lower than that of T_{CSI}.[2] The FC layers at the input and output have 16 and 32 hidden nodes, respectively. The LSTM uses the stacked cell states of size 32.

4) Training Procedure: A total of $3,000,000$ data examples were generated for training and 1,000,000 examples were used to evaluate the proposed beam tracking method. The parameters used to train the LSTM model is provided in Table I. We generate the training data using the following procedure:

- Channel generation: generate the length-10,000 sequences of AoA based on (26).
- Generation of IMU sensor measurements: generate the length-40,000 sequences of angular velocity and acceleration measurements by taking first and second derivatives of the AoA sequence. For each sequence, we add the Gaussian noise with a random SNR uniformly distributed in the range $[6, 15]$ dB.
- Training data generation: we partition the sequences of AoA into short sequence of length 4. The first three AoA states are used as inputs to the LSTM and the last AoA state is used as a label. Note that the sequences of the oversampled IMU sensor measurements are partitioned accordingly.

[2]In practical systems, IMU sensors operate independently with the channel tracking protocol, so the sampling period of IMU sensors is not necessarily identical to the beam transmission cycle T_{CSI}. We assume that the IMU sensor data is resampled to have K times lower sampling period than T_{CSI}. Larger K indicates higher granularity of the IMU data samples in the time domain, which makes it better to predict future channel states. Our experiments confirmed that the setting $K = 4$ leads to better performance than $K = 1$.

TABLE I
TRAINING CONFIGURATIONS OF LSTM MODEL

MINIBATCH	64
INITIAL_LEARNING_RATE	0.01
DECAY_EPOCH	3
DECAY_RATE	0.1
TOTAL_EPOCH	30
OPTIMIZER	Adam optimizer

B. Experimental Results

In this section, we compare our method with the following mmWave channel tracking methods:

1) Compressive channel tracking [16]: Orthogonal matching pursuit [41] followed by off-grid refinement was used to track the AoA.
2) EKF method [7]: The AoA was estimated using the EKF.
3) Least mean square (LMS) method [17]: The AoA was estimated by using the LMS filter.
4) LSTM based tracking [25]: The LSTM model directly estimates the AoA. It was trained using the cosine loss function.
5) ML-based training [26]: The LSTM model predicts the channel state which is used to determine the beamforming vector without pilot measurement.
6) Proposed (CSI) method: Only previous AoA estimates were used to predict the future channel state information (CSI). This method was evaluated to investigate the advantage of using IMU sensors for beam tracking.
7) Proposed (CSI+IMU) method: The previous AoA estimates and IMU measurements were used to predict the future channel distribution.

As the compressive channel tracking, LMS, and LSTM-based tracking methods do not produce the distribution of AoA, we used $M_m = 2$ beams closest to the previous AoA estimate as the Rx sounding beams. In contrast, like the proposed method, the EKF method yields the distribution of the AoA, which is used to determine the Rx sounding beams. The normalized mean square error (MSE) is defined as

$$MSE = 10\log_{10}\frac{\left\|\mathbf{H}_t - \hat{\mathbf{H}}_t\right\|_F^2}{\|\mathbf{H}_t\|_F^2}.$$

Fig. 6 shows the bit error rate (BER) performance as a function of SNR. The parameter a_{avg} indicates the extent of mobility of the UE. Fig. 6 (a), (b), and (c) show the performance curves for $a_{avg} = 0.1\pi$, 0.2π, and 0.4π, respectively. We observe that the proposed (CSI+IMU) method

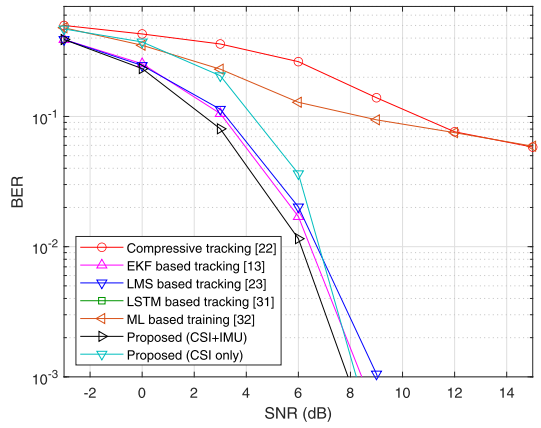

(a)

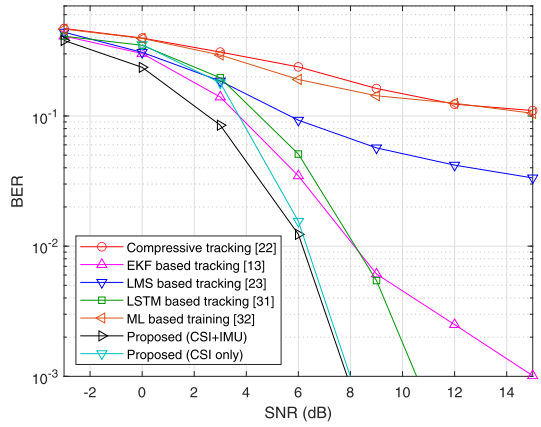

(b)

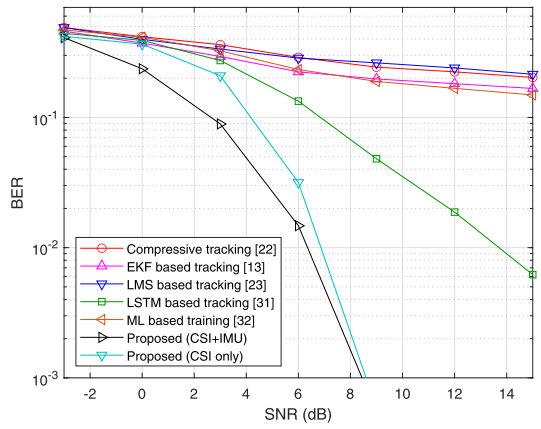

(c)

Fig. 6. BER versus SNR of several channel tracking methods for (a) $a_{avg} = 0.1\pi$, (b) $a_{avg} = 0.2\pi$, and (c) $a_{avg} = 0.4\pi$.

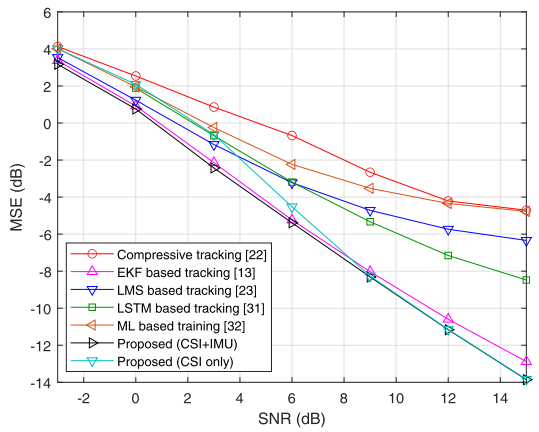

(a)

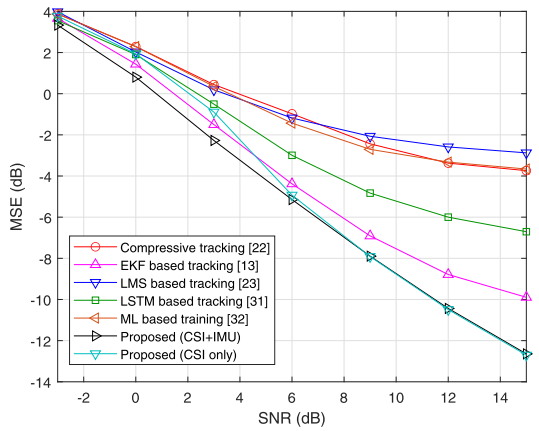

(b)

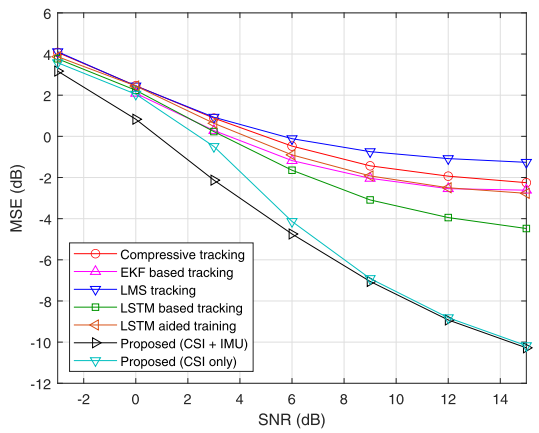

(c)

Fig. 7. Normalized MSE versus SNR of several channel tracking methods for (a) $a_{avg} = 0.1\pi$, (b) $a_{avg} = 0.2\pi$, and (c) $a_{avg} = 0.4\pi$.

outperforms the existing methods for all the cases considered. When a_{avg} is 0.1π rad/s, the proposed method achieves a performance gain of approximately 1 dB over the EKF method at the BER of 10^{-3}. As a_{avg} increases, the channel changes more dynamically and the performance gain of the proposed method increases. With $a_{avg} = 0.2\pi$, the proposed method achieves a gain of more than 3 dB over other algorithms. Furthermore, with $a_{avg} = 0.4\pi$, the performance gain increases up to more than 10 dB. This indicates that the LSTM-based channel model provides a more accurate model of time-varying AoAs, and thus, superior performance is achieved under higher mobility. Fig. 6 also shows the advantage of using IMU sensors for beam tracking. The proposed (CSI+IMU) method achieves a performance gain over the proposed (CSI) method, especially

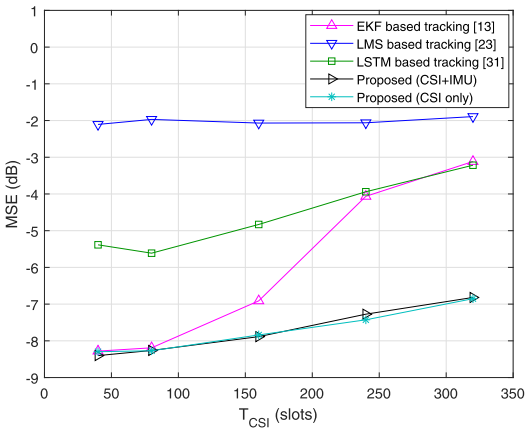

(a)

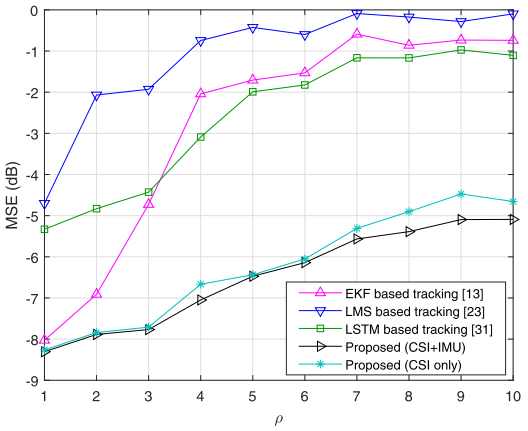

(b)

Fig. 8. Normalized MSE versus (a) T_{CSI} and (b) a_{avg}.

in the low SNR range. This appears to be because the channel estimates obtained in the previous beam transmission cycles would not be reliable in the low SNR range; thus, the IMU sensor signals can compensate the degraded channel estimation. Note that, although both the proposed and EKF methods perform the same measurement update step, the proposed method achieves a better performance owing to its more accurate prediction results in the prediction update step. Note also that, although both our method and the methods in [25], [26] employ DNN for beam tracking, the proposed method performs better by leveraging the underlying domain knowledge in the measurement model.

Fig. 7 shows the normalized MSE as a function of SNR for several beam tracking methods. The proposed method achieves a significant performance gain over the existing methods for all the cases considered. The performance gain of the proposed method also increases with a_{avg}. The proposed method can track rapidly varying channels better by using the DNN and IMU sensor measurements.

Fig. 8 illustrates the variation in the MSE performance with the beam transmission period T_{CSI} and the angular velocity a_{avg} when the SNR is set to 9 dB. Fig. 8 (a) shows the plot of MSE versus T_{CSI} when a_{avg} is fixed to 0.2π. As T_{CSI} increases, the sounding beams are transmitted less frequently, and the beam tracking method experiences larger channel variations. With a small T_{CSI}, the performance of the EKF method is comparable to that of the proposed method. However, the performance of the EKF method severely deteriorates with T_{CSI}, and consequently, the performance gap between these two methods increases rapidly. Fig. 8 (b) shows the plot of MSE versus a_{avg} when T_{CSI} is fixed to 160 slots. The performance of the beam tracking algorithms degrades as the channel changes more dynamically owing to the fast motion of the UE. As a_{avg} increases, the EKF method does not perform well because the linear channel model used in the EKF method does not sufficiently capture the behavior of time-varying channels. In contrast, the proposed method successfully models the complex channel behavior for reliable beam tracking.

VI. Conclusion

In this paper, we proposed a deep learning-based beam tracking method for mmWave communication. The proposed beam tracking method was designed to track fast-varying AoD and AoA due the motion of the UE device. We employed the LSTM to model the channel variation and predict the future distribution of the channel state based on the sequence of the previous channel estimates and IMU sensor measurements. Our method is based on a sequential Bayesian estimation framework, in which the prediction model yields the prior distribution of the channel in the prediction update step, and the predicted distribution is used to update the channel estimate in the measurement update step. Thus, our method is a hybrid approach in that we used both an LSTM-based channel model and an analytical measurement model for beam tracking. Our simulation results showed that the proposed method achieved a significant performance gain over the EKF baseline and outperformed the existing beam tracking methods, especially in high-mobility scenarios. Because both EKF and particle filter are widely used to solve nonlinear state estimation problems, it would be possible to apply our LSTM-based method to particle filters as well. This requires designing a way to draw and propagate particles through iterations, and LSTM-based predictors should be integrated into these particle filtering processes. This subject is left for the future work.

Appendix

A. Derivation of Jacobian Matrix

The Jacobian matrix $\mathbf{O}_t$ is expressed as

$$\mathbf{O}_t = \left[\frac{\partial q(\gamma_t)}{\partial \theta_{1,t}^{(b)}}, \frac{\partial q(\gamma_t)}{\partial \theta_{1,t}^{(m)}}, \ldots, \frac{\partial q(\gamma_t)}{\partial \theta_{L,t}^{(b)}}, \frac{\partial q(\gamma_t)}{\partial \theta_{L,t}^{(m)}} \right],$$

whose elements in the $(M(i-1)+j)$th row are given by

$$\frac{\partial q^{(M(i-1)+j)}}{\partial \theta_{l,t}^{(b)}} = \frac{\alpha_{l,t}}{n_t n_r} \frac{1-\epsilon_m^{(k_m N_m)}}{1-\epsilon_m^{(k_m)}} \times \frac{k_b \epsilon_b^{(k_b)} - k_b N_b \epsilon_b^{(k_b N_b)} - k_b (N_b - 1) \epsilon_b^{(k_b (N_b+1))}}{\left(1-\epsilon_b^{(k_b)}\right)^2}$$

$$\frac{\partial q^{(M(i-1)+j)}}{\partial \theta_{l,t}^{(m)}} = \frac{\alpha_{l,t}}{n_t n_r} \frac{1-\epsilon_b^{(k_b N_b)}}{1-\epsilon_b^{(k_b)}} \times \frac{k_m \epsilon_m^{(k_m)} - k_m N_m \epsilon_m^{(k_m N_m)} - k_m (N_m - 1)\epsilon_m^{(k_m (N_m+1))}}{\left(1-\epsilon_m^{(k_m)}\right)^2},$$

where $\epsilon_b = e^{(\theta_{l,t}^{(b)} - \nu_{t,i}^{(b)})}$, $\epsilon_m = e^{(\theta_{l,t}^{(m)} - \nu_{t,i}^{(m)})}$, $k_b = -\frac{j2\pi d_b}{\lambda}$ and $k_m = -\frac{j2\pi d_m}{\lambda}$.

REFERENCES

[1] T. S. Rappaport *et al.*, "Millimeter wave mobile communications for 5G cellular: It will work!" *IEEE Access*, vol. 1, pp. 335–349, May 2013.

[2] F. Boccardi, R. W. Heath, A. Lozano, T. L. Marzetta, and P. Popovski, "Five disruptive technology directions for 5G," *IEEE Commun. Mag.*, vol. 52, no. 2, pp. 74–80, Feb. 2014.

[3] A. Alkhateeb, O. El Ayach, G. Leus, and R. W. Heath, Jr., "Channel estimation and hybrid precoding for millimeter wave cellular systems," *IEEE J. Sel. Topics Signal Process.*, vol. 8, no. 5, pp. 831–846, Oct. 2014.

[4] W. Roh *et al.*, "Millimeter-wave beamforming as an enabling technology for 5G cellular communications: Theoretical feasibility and prototype results," *IEEE Commun. Mag.*, vol. 52, no. 2, pp. 106–113, Feb. 2014.

[5] S. Han, I. Chih-Lin, Z. Xu, and C. Rowell, "Large-scale antenna systems with hybrid analog and digital beamforming for millimeter wave 5G," *IEEE Commun. Mag.*, vol. 53, no. 1, pp. 186–194, Jan. 2015.

[6] Q. Duan, T. Kim, H. Huang, K. Liu, and G. Wang, "AoD and AoA tracking with directional sounding beam design for millimeter wave MIMO systems," in *Proc. IEEE 26th Annu. Int. Symp. Pers., Indoor, Mobile Radio Commun. (PIMRC)*, Aug./Sep. 2015, pp. 2271–2276.

[7] C. Zhang, D. Guo, and P. Fan, "Tracking angles of departure and arrival in a mobile millimeter wave channel," in *Proc. IEEE Int. Conf. Commun. (ICC)*, May 2016, pp. 1–6.

[8] V. Va, H. Vikalo, and R. W. Heath, "Beam tracking for mobile millimeter wave communication systems," in *Proc. IEEE Global Conf. Signal Inf. Process. (GlobalSIP)*, Dec. 2016, pp. 743–747.

[9] E. A. Wan and R. Van Der Merwe, "The unscented Kalman filter for nonlinear estimation," in *Proc. IEEE Adapt. Syst. Signal Process., Commun., Control Symp.*, Oct. 2000, pp. 153–158.

[10] S. G. Larew and D. J. Love, "Adaptive beam tracking with the unscented Kalman filter for millimeter wave communication," *IEEE Signal Process. Lett.*, vol. 26, no. 11, pp. 1658–1662, Nov. 2019.

[11] S. Jayaprakasam, X. Ma, J. W. Choi, and S. Kim, "Robust beam-tracking for mmWave mobile communications," *IEEE Commun. Lett.*, vol. 21, no. 12, pp. 2654–2657, Dec. 2017.

[12] J. Seo, Y. Sung, G. Lee, and D. Kim, "Training beam sequence design for millimeter-wave MIMO systems: A POMDP framework," *IEEE Trans. Signal Process.*, vol. 64, no. 5, pp. 1228–1242, Mar. 2016.

[13] J. W. Choi, B. Shim, Y. Ding, B. Rao, and D. I. Kim, "Compressed sensing for wireless communications: Useful tips and tricks," *IEEE Commun. Surveys Tuts.*, vol. 19, no. 3, pp. 1527–1550, 3rd Quart., 2017.

[14] J. Brady, N. Behdad, and A. M. Sayeed, "Beamspace MIMO for millimeter-wave communications: System architecture, modeling, analysis, and measurements," *IEEE Trans. Antennas Propag.*, vol. 61, no. 7, pp. 3814–3827, Jul. 2013.

[15] X. Gao, L. Dai, Y. Zhang, T. Xie, X. Dai, and Z. Wang, "Fast channel tracking for terahertz beamspace massive MIMO systems," *IEEE Trans. Veh. Technol.*, vol. 66, no. 7, pp. 5689–5696, Jul. 2017.

[16] Z. Marzi, D. Ramasamy, and U. Madhow, "Compressive channel estimation and tracking for large arrays in mm-wave picocells," *IEEE J. Sel. Topics Signal Process.*, vol. 10, no. 3, pp. 514–527, Apr. 2016.

[17] Y. Yapici and I. Guvenc, "Low-complexity adaptive beam and channel tracking for mobile mmWave communications," in *Proc. 52nd Asilomar Conf. Signals, Syst., Comput.*, Oct. 2018, pp. 572–576.

[18] J. Li, Y. Sun, L. Xiao, S. Zhou, and C. Emre Koksal, "Fast analog beam tracking in phased antenna arrays: Theory and performance," 2017, *arXiv:1710.07873*. [Online]. Available: http://arxiv.org/abs/1710.07873

[19] J. Bao, D. Sun, and H. Li, "Motion sensor aided beam tracking in mobile devices of millimeter-wave communications," in *Proc. IEEE Int. Conf. Commun. (ICC)*, May 2018, pp. 1–7.

[20] M. Brambilla, M. Nicoli, S. Savaresi, and U. Spagnolini, "Inertial sensor aided mmWave beam tracking to support cooperative autonomous driving," in *Proc. IEEE Int. Conf. Commun. Workshops (ICC Workshops)*, May 2019, pp. 1–6.

[21] Y. Lin, C. Shen, and Z. Zhong, "Sensor-aided predictive beam tracking for mmWave phased array antennas," in *Proc. IEEE Globecom Workshops (GC Wkshps)*, Dec. 2019, pp. 1–5.

[22] C.-H. Wang, T. Shimizu, H. Muralidharan, and A. Yamamuro, "Demo: A real-time high-definition vehicular sensor data sharing system using millimeter wave V2 V communications," in *Proc. IEEE Veh. Netw. Conf. (VNC)*, Dec. 2020, pp. 1–2.

[23] Y. LeCun, Y. Bengio, and G. Hinton, "Deep learning," *Nature*, vol. 521, no. 7553, p. 436, May 2015.

[24] A. M. Elbir, K. Vijay Mishra, M. R. Bhavani Shankar, and B. Ottersten, "A family of deep learning architectures for channel estimation and hybrid beamforming in multi-carrier mm-wave massive MIMO," 2019, *arXiv:1912.10036*. [Online]. Available: http://arxiv.org/abs/1912.10036

[25] D. Burghal, N. A. Abbasi, and A. F. Molisch, "A machine learning solution for beam tracking in mmWave systems," in *Proc. 53rd Asilomar Conf. Signals, Syst., Comput.*, Nov. 2019, pp. 173–177.

[26] Y. Guo, Z. Wang, M. Li, and Q. Liu, "Machine learning based mmWave channel tracking in vehicular scenario," in *Proc. IEEE Int. Conf. Commun. Workshops (ICC Workshops)*, May 2019, pp. 1–6.

[27] Y. Long, Z. Chen, and S. Murphy, "Broad learning based hybrid beamforming for mm-wave MIMO in time-varying environments," *IEEE Commun. Lett.*, vol. 24, no. 2, pp. 358–361, Feb. 2020.

[28] Y. Yang, S. Zhang, F. Gao, J. Ma, and O. A. Dobre, "Graph neural network-based channel tracking for massive MIMO networks," *IEEE Commun. Lett.*, vol. 24, no. 8, pp. 1747–1751, Aug. 2020.

[29] M. Giordani, M. Mezzavilla, and M. Zorzi, "Initial access in 5G mmWave cellular networks," *IEEE Commun. Mag.*, vol. 54, no. 11, pp. 40–47, Nov. 2016.

[30] R. W. Heath, N. González-Prelcic, S. Rangan, W. Roh, and A. M. Sayeed, "An overview of signal processing techniques for millimeter wave MIMO systems," *IEEE J. Sel. Topics Signal Process.*, vol. 10, no. 3, pp. 436–453, Apr. 2016.

[31] Z. Xiao, T. He, P. Xia, and X.-G. Xia, "Hierarchical codebook design for beamforming training in millimeter-wave communication," *IEEE Trans. Wireless Commun.*, vol. 15, no. 5, pp. 3380–3392, May 2016.

[32] Y. M. Tsang, A. S. Y. Poon, and S. Addepalli, "Coding the beams: Improving beamforming training in mmwave communication system," in *Proc. IEEE Global Telecommun. Conf. (GLOBECOM)*, Dec. 2011, pp. 1–6.

[33] W. Yuan, S. M. D. Armour, and A. Doufexi, "An efficient and low-complexity beam training technique for mmWave communication," in *Proc. IEEE 26th Annu. Int. Symp. Pers., Indoor, Mobile Radio Commun. (PIMRC)*, Aug. 2015, pp. 303–308.

[34] J. Wang *et al.*, "Beam codebook based beamforming protocol for multi-Gbps millimeter-wave WPAN systems," *IEEE J. Sel. Areas Commun.*, vol. 27, no. 8, pp. 1390–1399, Oct. 2009.

[35] *NR; Physical Channels and Modulation (Release 15)*, 3rd Generation Partnership Project (3GPP), document 3GPP TS 38.211 V15.2.0, 2018.

[36] S. Hochreiter and J. Schmidhuber, "Long short-term memory," *Neural Comput.*, vol. 9, no. 8, pp. 1735–1780, Nov. 1997.

[37] Z. Guo, X. Wang, and W. Heng, "Millimeter-wave channel estimation based on 2-D beamspace MUSIC method," *IEEE Trans. Wireless Commun.*, vol. 16, no. 8, pp. 5384–5394, Aug. 2017.

[38] D. P. Kingma and J. Ba, "Adam: A method for stochastic optimization," 2014, *arXiv:1412.6980*. [Online]. Available: http://arxiv.org/abs/1412.6980

[39] S. J. Julier, "The scaled unscented transformation," in *Proc. Amer. Control Conf.*, vol. 6, May 2002, pp. 4555–4559.

[40] S. H. Lim, S. Kim, B. Shim, and J. W. Choi, "Efficient beam training and sparse channel estimation for millimeter wave communications under mobility," *IEEE Trans. Commun.*, vol. 68, no. 10, pp. 6583–6596, Oct. 2020.

[41] J. A. Tropp and A. C. Gilbert, "Signal recovery from random measurements via orthogonal matching pursuit," *IEEE Trans. Inf. Theory*, vol. 53, no. 12, pp. 4655–4666, Dec. 2007.

Sun Hong Lim (Member, IEEE) received the B.S. degree from the Department of Electrical Engineering, Hanyang University, Seoul, South Korea, in 2016, where he is currently pursuing the Ph.D. degree in electrical engineering. His research interests include signal processing, compressed sensing, wireless communications, and machine learning.

Sunwoo Kim (Senior Member, IEEE) received the B.S. degree from Hanyang University, Seoul, South Korea, in 1999, and the Ph.D. degree from the Department of Electrical and Computer Engineering, University of California, Santa Barbara, in 2005. Since 2005, he has been working with the Department of Electronic Engineering, Hanyang University, where he is currently a Professor. He was a Visiting Scholar with the Laboratory for Information and Decision Systems, Massachusetts Institute of Technology, from 2018 to 2019. He is also the Director of the 5G/Unmanned Vehicle Research Center, funded by the Ministry of Science and ICT, South Korea. His research interests include wireless communication/positioning/localization, and statistical signal processing. He is also an Associate Editor of IEEE TRANSACTIONS ON VEHICULAR TECHNOLOGY.

Byonghyo Shim (Senior Member, IEEE) received the B.S. and M.S. degrees in control and instrumentation engineering from Seoul National University (SNU), South Korea, in 1995 and 1997, respectively, and the M.S. degree in mathematics and the Ph.D. degree in electrical and computer engineering from the University of Illinois at Urbana–Champaign (UIUC), Champaign, IL, USA, in 2004 and 2005, respectively. From 1997 to 2000, he was an Officer (first lieutenant) and an academic full-time Instructor with the Department of Electronics Engineering, Korean Air Force Academy. From 2005 to 2007, he was a Staff Engineer with Qualcomm Inc., San Diego, CA, USA. From 2007 to 2014, he was an Associate Professor with the School of Information and Communication, Korea University, Seoul. Since 2014, he has been with SNU, where he is currently a Professor and the Vice Chair of the Department of Electrical and Computer Engineering. His research interests include wireless communications, statistical signal processing, compressed sensing, and machine learning. He is an Elected Member of the Signal Processing for Communications and Networking (SPCOM) Technical Committee of the IEEE Signal Processing Society. He was a recipient of M. E. Van Valkenburg Research Award from the Department of ECE, University of Illinois, in 2005; Hadong Young Engineer Award from IEIE in 2010; Irwin Jacobs Award from Qualcomm and KICS in 2016; Shinyang Research Award from the Engineering College of SNU in 2017; and Okawa Foundation Research Award in 2020. He served as an Associate Editor for IEEE TRANSACTIONS ON SIGNAL PROCESSING, IEEE TRANSACTIONS ON COMMUNICATIONS, IEEE TRANSACTIONS ON VEHICULAR TECHNOLOGY, IEEE WIRELESS COMMUNICATIONS LETTERS, and *Journal of Communications and Networks*, and a Guest Editor for IEEE JOURNAL ON SELECTED AREAS IN COMMUNICATIONS.

Jun Won Choi (Member, IEEE) received the B.S. and M.S. degrees from the Department of Electrical Engineering, Seoul National University, and the Ph.D. degree in electrical and computer engineering from the University of Illinois at Urbana–Champaign. In 2010, he joined Qualcomm Inc., San Diego, USA, where he participated in the research on advanced signal processing technology for next generation wireless systems. In 2013, he joined the Department of Electrical Engineering, Hanyang University, as a Faculty Member. His research areas include signal processing, machine learning, intelligent vehicles, and wireless communications. He served as an Associate Editor for IEEE TRANSACTIONS ON VEHICULAR TECHNOLOGY and IEEE TRANSACTIONS ON INTELLIGENT TRANSPORTATION SYSTEMS.